The Use of Soft Lithography to Reproduce Snail-Like Movement by Creating Pressure Gradients in Thin Films

by

Pey-Hua B. Hwang

SUBMITTED TO THE DEPARTMENT OF MECHANICAL ENGINEERING
IN PARTIAL FULFILLMENT OF THE REQUIREMENTS
FOR THE DEGREE OF

BACHELOR OF SCIENCE IN MECHANICAL ENGINEERING

AT THE

MASSACHUSSETS INSTITUTE OF TECHNOLOGY

June 2004

Copyright 2004 Pey-Hua B. Hwang
All rights reserved.
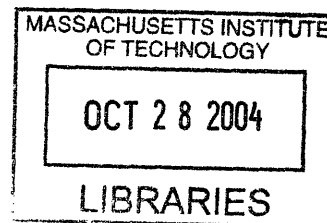
Signature of Author:_____
Department of Mechanical Engineering
May 7, 2004

Certified by: _____
Anette E. Hosoi
Assistant Professor of Mechanical Engineering
Thesis Supervisor

Accepted by:_____
Ernest G. Cravalho
Professor of Mechanical Engineering
Chairman of the Undergraduate Thesis Committee

1

The Use of Soft Lithography to Reproduce Snail-Like Movement by Creating Pressure Gradients in Thin Films

by

Pey-Hua B. Hwang

Submitted to the Department of Mechanical Engineering
on May 7, 2004 in Partial Fulfillment of the
Requirements for the Degree of Bachelor of Science in
Mechanical Engineering

ABSTRACT

By imitating nature, man finds ways to expand his capacities. To achieve this aim, he often takes natures designs, simplifies them to their most basic principles and then works in a retrograde fashion to add back the complexity originally stripped away to make the first discoveries. This thesis is based on previous work done on modeling snail movement on a macroscopic scale using a motor driven wave propagation machine. This project scaled down the mechanism to a size more commonly found in nature. This downscaling required a new method for producing waves. Peristaltic pumping achieved through the use of soft-lithography and pneumatics was the method chosen. This combination of ideas proved challenging for several reasons. First, the pumping method had previously only been used with one channel per pneumatic input, whereas the snail required each input to feed a multitude of branching channels creating a more complicated fluid dynamics problem. Second, the snail waves were downscaled from a continuous sinusoid to the three phase stepping mechanism of the peristaltic pump. Each three-phase cycle was considered equivalent to one wavelength. Thus, after creating a design that could move, the ratio between the traveling wavelength speed and subsequent net movement were compared to the aforementioned mathematical model. The model's ratio was 0.56 net/wave velocity. The actual ratio was .05 net/wave velocity. The difference by an order of magnitude could be attributed to the discontinuity of the pumping mechanism as opposed to the continuous nature of an actual traveling wave.

Thesis Supervisor: Anette E. Hosoi
Title: Assistant Professor of Mechanical Engineering

1.0 Introduction

Currently, many scientific advances come in the form of taking machines and making them smaller. Machines that involve locomotion often derive inspiration from animal movement. While animals may achieve net motion forwards at fairly constant velocities, the forces they exert on the environment are anything but constant. An overriding theme of animal locomotion is that propulsive forces vary with time and that kinetic energy can be stored in many different forms. For small organisms, viscous resistances in fluid can produce motion of the organism relative to the fluid as long as the organism's motion is asymmetric. [4] The organism in question for this thesis is the snail and its relative the slug. Bridging from work in modeling snail movement on the large scale, it made sense to apply this model that involved the variance of pressure gradients to a smaller scale that would more closely mimic the biological size scale and mechanical motion equivalent of slug and snail movement.[3]

1.1 Snail and Slug Movement Through Continuous Wave Propagation

Locomotion in snails, slugs and limpets is different from locomotion in other animals. Because they have only one foot, the great majority of them adhere to the surface on which they crawl, and from the dorsal view they appear to move without moving parts. The explanation of the adherence and gliding movement is found in two factors. The presence of mucus, and the waves that move in series along the ventral, also known as the pedal, portion of the foot work together to create forward locomotion. [1]

In some snails, the waves move from the posterior to the anterior of the snail in the same direction as the net snail movement. This type of wave is called a direct wave. In other snails the waves move from the anterior to the posterior of the snail in the opposite direction of the net snail movement. This sort of wave is termed a retrograde wave. These waves cause forward motion by inducing various forces in the mucus. Thus, studying these forces and their reactions as the pedal wave moves can lead to better understandings of the mechanisms involved in gastropod locomotion. [1] In this study, viscous fluid is used instead of mucous to simplify modeling and focus on the pressure dependent aspects of the velocity due to wave propagation.

1.2 Peristaltic Pump Induction of Fluid Movement

In multilayer soft lithography multilayer structures are constructed by bonding layer of elastomer. Each of these layers is separately cast from micro-machined molds. Each layer has an excess of one of the two component reactive molecules. When the layers are interfaced the excess molecules on one side of the interface bond with the excess of the other component molecules on the other side of the interface; thus, further curing causes the two layers to irreversibly bond. Much like a good weld joint is as strong as the component parts it's joining, the strength of this interface equals the strength of the bulk elastomer. Most importantly for the actuation of microstructures, the elastomer is a soft material with a Young's modulus of approximately 750kPa allowing large deflections with small actuation forces. Monolithic elastomer valves can be actuated with speeds that allow for opening and closing at 100Hz and a time response of 1 ms. Peristaltic pumps are formed by arranging three valves on a single

3

channel. [6] As these valves are opened and closed fluids can be forced through the channel. By imitating this asymmetric deflection of fluid it was hoped to approximate the sinusoidal traveling waves found on the underbellies of slugs. Essentially, it was hoped that the peristaltic pumping would move the fluid layer underneath the snail in the same way it could move fluid through a small channel and create a moving pneumatic snail.

2.0 Theory

2.1 Using modeling to determine snail velocity

Using MATLAB and Dev C++ programming it is possible to model the velocity of snail movement relative to wave movement. The programming code developed by Susan Ji found in Appendix A approximated the gap between the snail foot and the ground as a lubrication layer, and used formulas for the velocity, pressure, and force values which were derived from the Navier-Stokes equations. This program was then used to determine scaling parameters for the smaller snail.

The original robosnail was approximately three times larger than the scaled down parameters found from running the code. In Table 1 below is a comparison of the original snail dimensions and the parameters used in the first iteration of snail making.

Table 1: Comparison of Original Snail and Scaled Down Snail Parameters

	Original Robosnail	New Snail Parameters
Traveling Wavelength	4.572 cm	1.4cm
Wave Amplitude	.1778 cm	0.01cm
Velocity of Wave	1.778cm/s	.1cm/s
Mass of Snail	125.438g	1.5g
Width of Snail	3.2512cm	1.4cm
Length of Snail	13.97cm	4.4cm
Height of Snail	2.59cm	1cm
Predicted Velocity of Snail	0.5 cm/s	0.056cm/s

2.2 Inflationary pressure inside the channels

The Microsnail crawling on thin films using pneumatic pumping is essentially a compound fluids problem because the fluid being pumped through the channels is subject to pressure drop due to frictional losses due to channel length. Secondly, because this pressure drop is directly related to the amount of force exerted on the flexible membrane of the channels it also influences the amount of deflection in any one part of the membrane thus the pressure drop could essentially reduce any possibly deflection to an essentially negligible amount. The simplest model found was one that modeled the fluid rushing into the sealed channels at high pressures, and compressing the air in the channels. This system thus, was modeled using the Bernoulli equation that included head loss as shown in Equation 1:

$$\left[\frac{P}{\rho g} + \frac{v^2}{2g} + z\right]_{in} = \left[\frac{P}{\rho g} + \frac{v^2}{2g} + z\right]_{out} + h_{friction} \qquad (1)$$

where v represents the velocity of the fluid, P represents the pressure of the fluid, ρ represents the density of the fluid, z represents the height of the fluid, g represents the gravitational constant, and $h_{friction}$ represents the losses due to friction. Since all of the terms on both sides of the equation with the exception of P were constant this equation could be used to solve for pressure loss. There were several main factors in determining $h_{friction}$. These factors were plugged into Equation 2:

$$h_{friction} = \frac{128\mu LQ}{\pi \rho g d^4} \qquad (2)$$

where μ was the viscosity of the fluid, L was the length the fluid had to travel(channel length), Q was fluid flow rate, and d was the wetted perimeter of the fluid. [5] Because it was not possible to measure the fluid flow rate directly $h_{friction}$ was found through an iterative process that first took the pressure drop to be complete from input pressure to zero at the end of the channel. The flow rate was then calculated, adjusted in accordance to observation of actual channel fill and plugged back into equation one to find a new pressure drop. Unfortunately, this theory resulted in generally unreasonable flow rates above 30m/s and thereby was abandoned in favor of an experimental approach to determine the optimum fill pressure for the channels which is explained in Section 3.2.3.

The deflection in the elastomeric material was related to the amount of stress in the channels. Since the upper mold was of a thickness that it behaved as a rigid structure only the membrane stretched over the channels would react by inflating. Essentially, the channel layer which ranged from 0.5 cm to 0.75cm thick was over 1000 times thicker than the membrane layer which was 40 microns or 0.0004cm.

The amount of inflation could be related to the pressure applied through the Equations 3, 4, 5, and 6. First, pressure applied was related to strain by the constituitive relation found in Equation 3[6]:

$$\sigma = E\varepsilon \qquad (3)$$

where σ was the applied pressure, E was the young's modulus, and ε was the strain.
Strain was then related to deflection by Equation 4:

$$\varepsilon = \delta / w \qquad (4)$$

where w was the width of the channel and δ was the deflection. Another method of measuring deflection would be to convert the pressure into a distributed force. The relationship between pressure and force is displayed in Equation 5:

$$F = \sigma * A \qquad (5)$$

where F was the force and A was the area over which the pressure was applied. The force could then be plugged into the equation for beam bending of a beam constrained on either side with a force applied in its center as shown in Equation 6:

$$\delta = \frac{F}{L} * \frac{x}{24EI}(w^3 - 2wx^2 - x^3) \tag{6}$$

where L was the length of the channel making F/L the load per unit length along the deflecting width of the channel, and x was the distance from one edge of the channel at which one wanted to calculate the deflection, and I was the moment of inertia of the membrane that could modeled as a rectangular beam with the cross section parameters taken from the thickness of the membrane and the length of the channel.[6] This approach would neglect edge effects on either end of the channel lengths. This simplification is possible because, in comparison, the length of the channel is much greater than the width of the channel.

3.0 Experimental Apparatus and Methods

3.1 Apparatus

There was a significant amount of lab equipment ranging from bench-top, to fume-hood, to clean room necessary to create and run the pneumatic powered snail.

3.1.1 Designing the Snail

The design for the snail was mostly focused on the channel pattern for the peristaltic pumping that would be used to drive the snail forwards. Because this pattern was essentially 2-D Adobe Illustrator 10.0 run on a Dell computer was used to create photolithography mask patterns. These patterns were then sent to a specialized printing company, Mika Color, to create the transparencies or masks that would eventually be used to build the snail. A sample mask for a positive photoresist and a sample for a negative photoresist mask can be found in Section 4.0 where results and design are discussed.

3.1.2 Snail Building Equipment

To build the microsnail the molds had to be created. The molds were created using a photolithography process that required an acid hood approved spincoater with appropriate waste removal capacities for producing the appropriate thicknesses of photo-resist to be processed, a lightsource for activating the photo-resist, ovens or heating platforms for baking the activated photo-resist, and a fume hood for developing, cleaning, and drying the finished mold. Stainless steel tongs were used for handling the wafer plates to avoid contamination. Finally, the whole mold making process was done in a clean room.

After the mold process was finished the molds were placed in foil lined Petri dishes and the mixed elastomeric material was poured in the dish. The elastomer and catalyst were mixed using a Thinky supermixer. The exact mix ratios are detailed in Appendix B. This mold would produce the first half of the snail. The second half of the snail was produced with a

different elastomeric ratio mixture than the channel layer. This mixture was spincoated onto a blank silicon wafer using an ordinary (did not require acid hood capacities) spincoater. A fume hood was used to coat the silicon wafers in an adhesion prevention layer of either chlorotrimethylsilane or perfluoroctylsilane to prevent the elastomer from getting stuck to the molds.

Different mold parameters sometimes caused air bubbles to get trapped in the mold channels so a vacuum chamber was used to bring air bubbles to the surface of the elastomeric mix before baking. This bubble removal allowed the active channel portion of the mold to maintain its integrity.

3.1.3 Pneumatic Set Up

Once the snails completed production a separate set up was used to pump various fluids through the elastomeric channels. This pumping was accomplished by using a valve system which was connected to tanks of pressurized air was controlled by a circuit board. The circuit board was controlled by a Dell computer and the relevant accompanying programming was written by Mats Howard Cooper, a graduate student in the Hatsopoulos Microfluids Laboratory who had worked on applying peristaltic pumping for other uses, through the software Labview 6.1. Further details on the capabilities of the Labview program used to control the valve pumping of the snail can be found in Appendix C.

The valve system was attached to a pressurized air system which consisted of pressurized air tanks, an initial air flow valve, a pressure regulator, the Labview controlled valves, and finally the tubing that connected to the snail. The flow diagram found in Figure 1 below traces the path of the air.
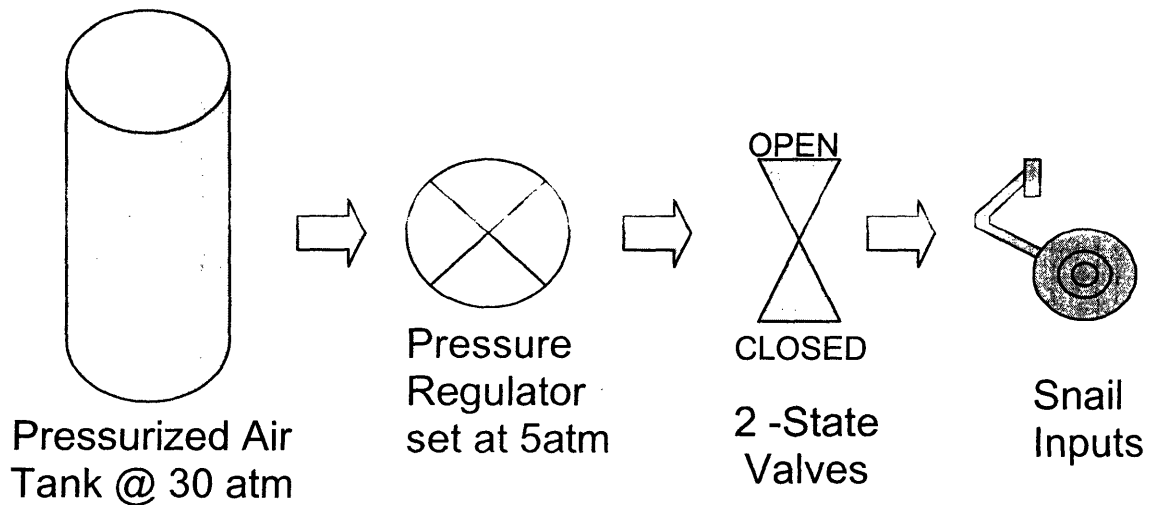

Figure 1: Airflow path schematic

3.2 Methods

This project entailed several iterations of design thus the processes for making and running the snails varied between the different iterations. The snail manufacturing process depended the most on the dimension sizes of the various channels because the thickness of photoresist needed to be kept at a ratio of at least 1:10 with the channel width. For example, if the channel width was 500 microns the photo resist needed to be at least 50 microns thick to avoid collapsing of channels during the assembly process between channel and membrane layers. Certain types of photoresist were optimized for specific ranges of thickness so the methods for mold creation had to be varied. Afterwards, when testing the snails the wetting properties of the viscous liquids on which it was run and the permeability of the elastomeric material became causes for methodology changes as well.

3.2.1 Making Snails

Making the snails was a multi-step process because it involved mold making, elastomer preparation, further processing of molded designs, and assembly of the completed pieces.

3.2.1.1 Making Snail Molds

Two types of snail molds were made due to different design constraints. The first set of molds was made using the positive photoresist AZ4620. A positive photo-resist uses a mask with the actual design in black to prevent exposure as noted in Section 3.1. After exposure, the developer then removes the exposed material. This photoresist, AZ4620, was chosen because of its high accuracy at a ten micron thickness. The general standard operating procedures followed can be found in reference 12. However, the specific procedures followed are as follows.

First the silicon wafers were cleaned using a series of solvents. The wafer was first given a rinsing of acetone, followed immediately by a rinse of isoproponal and finally by distilled water. The water was removed by forcing a stream of pressurized air over the wafer. All of these cleaning wafer preparation steps were done in the fume hood. An alternate method of wafer preparation would be to places the wafer on the spin coater and then all the fluids would be removed by the centrifugal forces on the spinning wafer, thereby eliminating the pressurized air step.

After the wafers were clean, they were placed on the spin coater and a layer of photoresist adhesion promoter was spread on silicon. After the adhesion promoter was spun on, a layer of photoresist was spun onto the wafer. The wafer was spun at 1500 rpm to achieve the 10 micron thickness required for proper exposure and development of the first mold design. The photoresist application was followed by a 1 hour prebake in a 90 degree centigrade oven. After the prebake, the wafer was placed in a KS-aligner, the photo-lithography mask was placed ink side down on top of the wafer, a heavy glass slide was placed on top of the mask to sandwich the mask onto the wafer and the whole assembly was

exposed to UV light for forty seconds. After the exposure the wafers were again placed in the fume hood and developed with 440 solution also know as specialized soapy water specifically designed to remove the exposed photoresist. This procedure required agitating the wafers in a shallow glass dish containing the 440 solution until all of the exposed photoresist was removed. The developing was considered finished when the wafer had reacquired its original mirror-like finish and the mold design was clear and apparent. The wafer was then removed from the 440 solution, rinsed in sequence with isopropanol and water, dried with the pressurized air. It was then inspected with a surface profilometer to double check mold integrity. The profilometer measured the height of the photoresist in comparison to the rest of the wafer to insure that the mold features were of uniform height.

When the design was changed to necessitate higher mold height differentials and a thicker layer of photoresist, the photoresist of choice became the negative photoresist SU-8 2050 whose developer removed unexposed material. General developing procedures can be found in reference 13; however, the exact method followed is detailed below.

The wafers were cleaned using the same methods as when using the positive photoresist. Next the adhesion promoter step was skipped and the wafer was directly spincoated with the SU-8. In order to achieve a feature height of 100 microns the spincoater was spun at 1700rpm. The wafer was then transferred to a hotplate set at 65 degrees centigrade for a 4 minute prebake. After the prebake, it was transferred to a 90 degree centigrade oven to bake for another 15 minutes. After the fifteen minutes it was transferred to the aligner, covered with the mask and glass coverslip in the same fashion as the negative photoresist, and exposed for 1 minute and 30 seconds. Following the exposure it was given a 8 minute postbake in the 65 degrees centigrade oven and then developed using a specialized SU-8 developer followed by isoproponal, water, and pressurized air rinses.

3.2.1.2 Fabrication and Assembly of the Snail

Fabricating the snail from the wafer molds involved two sets of steps. The first set of steps only needed to be followed once to prepare the molds, and subsequent snails would only need to follow the second set of steps.

For the first time preparation of the molds, a Petri dish was lined with aluminum foil. The mold was then placed within the lined dish and taken to the fume hood for a nonadhesive coating of either chlorotrimethylsilane or perfluoroctylsilane. This coating was achieved by placing a few drops of the chemical in a larger Petri dish. Then the smaller, uncovered foil-lined Petri containing the mold was placed next to the pool of chemical and the larger Petri was covered. The chemical was highly volatile so convection would vaporize the chemical and distribute the lubricating particles over the open Petri dish, thereby coating the wafer. The whole process took about one minute and thirty seconds for each wafer to be coated.

After wafer preparation the channel layer elastomeric mix had to be prepared. The products used and mix ratios are found in Appendix B. For covering a new mold about 30g of mix had to prepared for the channel side. This mix was measured out using a balance and then actually mixed in a Thinky Super Mixer. The Thinky Super Mixer had two settings. One for

9

mixing and one for degassing. Both functions were critical for ensuring that the catalyst and elastomer were uniformly distributed in the mix and that bubbles in the mix would not interfere with mold features. The mixing function was run for one minutes and the degassing feature for 2 minutes, per cup of elastomer mixed.

After the mix was prepared it was poured over the prepared wafer and then placed in an 80 degree centigrade oven to bake for 15 minutes. After the bake time was finished the channel layer was removed from the mold using an exacto knife or razor and a luer stub was used to punch the pneumatic input holes in the appropriate locations. A cross section of the finished channel layer would look approximately like Figure 2.
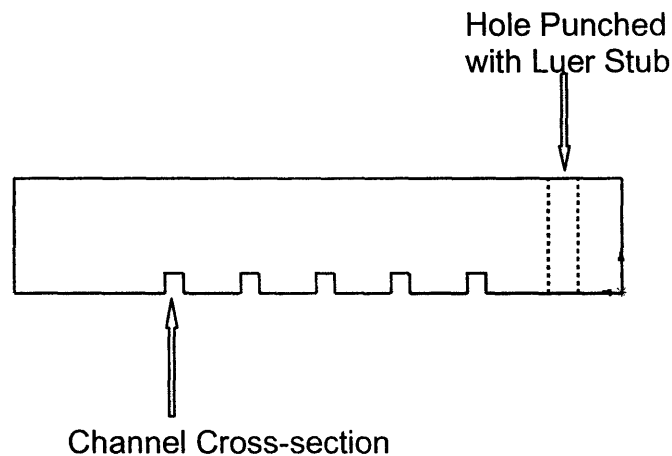
Hole Punched
with Luer Stub

Channel Cross-section

Figure 2: Representation of channel layer cross section lengthwise to convey how the air reaches the lower layer through a Luer Stub hole. This figure is not to scale nor does it represent the actual layout of the channels.

To create the membrane layer, a blank silicon wafer was cleaned using isoproponal and water. Next it was coated with the same nonadhesive layer as the molds. Next an elastomeric mix was spincoated on at a thickness of 30 microns on the spincoater which was set to ramp up to speed for 15 seconds and maintain that speed for 30 seconds. The bake time on the membrane layer occurred in the same 80 degree centigrade oven as the channel layer but could bake as little as 10 minutes before it was ready for use. The elastomer used was commonly referred to as PDMS or Poly-Dimethyl-Siloxan.

The channel layer with punched holes would then be laid on top of the membrane layer and the differential ratios of catalyst and elastomer in the two layers would bond to form a final assembled snail. An assembly of a channel and membrane layer with one luerstub hole is displayed in Figure 3. Actual snails have three Luer Stub holes for the three phase peristaltic pumping and the channels are looped accordingly. Again, this figure is merely to convey how the channel layer and membrane layer fuse to form a closed channel system with the only input at the luer stub hole.

Note that the Thickness of the channel layer is much greater than the membrane layer

Enclosed channels formed by membrane and channel layer

Luer Stub Hole

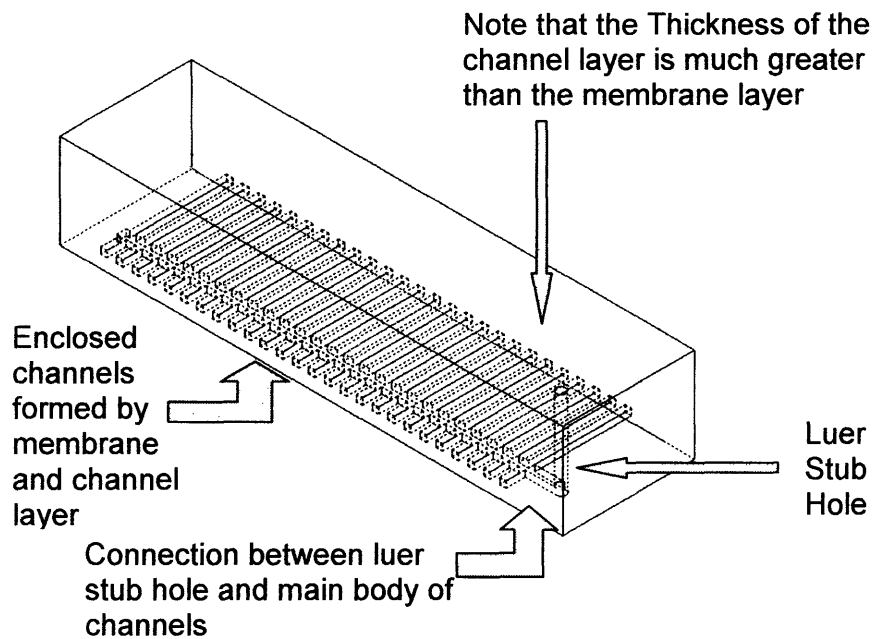Connection between luer stub hole and main body of channels

Figure 3: Channel and membrane layer assembly schematic

This assembly was first baked for only two hours during the first iteration of snail making; however, lack of proper adhesion between the layers due to the short bake resulted in a change of procedure for all subsequent snails. These snails were baked overnight at 80 degrees centrigrade to insure adequate bonding. Bonding complete, the membrane was cut away from the mold using either an exacto knife or razor blade, and the whole snail was peeled off the silicon wafer. The snail was then ready to be tested.

For subsequent snails, only about 18 grams of elastomeric mix had to be prepared to fill the mold where the previous snails were removed since the rest of the petri dish mold was already filled by the first batch of snail's extra elastomer. The non-adhesion layer step was unchanged for every batch process; though, because the non-adhesive particles did not remain on the wafer mold after each set of snails was released.

3.2.2 Running Snails

To run the snails was a multi-step procedure. First the snail had to be placed in a Petri dish with a thin coating of silicon oil. Next, the three input lines were filled with water to which had been added several drops of food coloring for better observation of channel filling. These lines were then connected to the valves and the snail inputs. Next the pressurized-air tank was opened and the pressure regulator was set to 5atm the previously determined optimal channel filling pressure discussed in Section 3.2.3. Finally, Labview was activated and the peristaltic program was run. The peristaltic program allowed for different valve switching speeds which allowed the channels to remain inflated for variable amounts of time

11

individually, and concurrently. The running speeds, duty cycle changes, and the effect on snail crawling speed are discussed in Section 4.4.

3.2.3 Determining Optimal Pressure for Running Snails

One of the problems encountered while running the snails was adequate inflation. Since inflation was a result of pressure the following procedure was used to determine optimal inflation pressure. First, the snail was set up in the usual running configuration. Next the pressure regulators were set to the minimum accurate pressure reading of 2atm. Below 2 atm there was difficulty in making accurate adjustments to the pressure. Labview was then activated to begin pumping the snail channels. The amount of fill in each channel was observed and then the pressure was increase by half an atmosphere. This testing continued until the level of 13 atm was reached. The failure value of the valves was 15 atm thereby the precaution to not exceed that value had to be taken.

4.0 Results and Design

The microsnail went through several iterations of design as the material properties and structural limitations of the elastomeric material were discovered.

4.1 Microsnail Iteration I

The first design iteration was a three phase snail with a design layout as displayed in Figure 4:
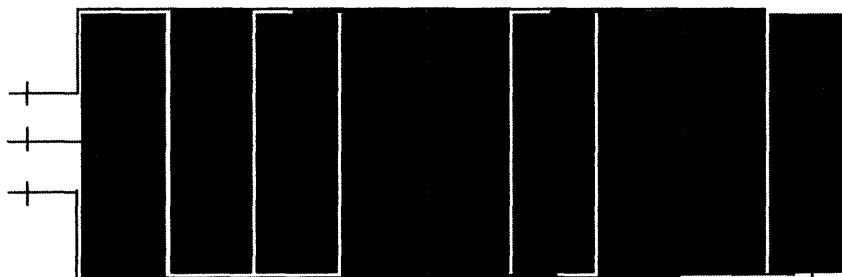
Figure 4: The positive photoresist mask of the three input snail. This figure is about twice as large as the actual snail for the purposes of clarity. The luer stub hole connects to the crosses on the left most end of the snail.

with an overall length of about 5 cm and over all width of about 1.5 cm. These centimeter dimensions had variation since each snail was hand cut off the mold with a razor and thereby the dimensions were not perfectly precise. The snail had three input channels that branched into series of channels that were arranged in pads. The hope was that the small channels would simultaneously inflate as units and thus create the shallow wave necessary to drive the snail forwards. Unfortunately, the first attempt at snail creation revealed that an inadequate baking time of a couple hours after the two layers had been assembled lead to adhesion

problems between the membrane and channel layers. Subsequent snails were built with an overnight bake time between the two layers. This time increase for crosslinking between layers resolved the adhesion problems.

However, there were still other issues to be resolved. Air was still being pumped through the channels and it was found that the elastomer was gas porous so there was gas leakage through diffusion that resulted in bubbles forming in the liquid film the snail was supposed to be moving over. Bubble creation aside there was no observable movement of the snail in any direction. First, the thin liquid layer the channel was tested as an area for concern since the glycerin used tended to pull away from the Petri dish edges in which the snail was being run creating an uneven surface. Unfortunately, when silicon oil, a liquid more conducive to wetting, was used there was still no observable snail movement.

Further inspection underneath a microscope revealed that the channels inflated slightly but a finger test over the active surface could not detect any deflection in the membrane. The one exception to this observation was at the input holes for the pneumatic insertion where there was an approximately 500 micrometer diameter circle of elastomer free to deflect there was finger detectable deflection. Additionally, when the snail was flipped upside down and a glass slide was placed over a thin layer of silicon oil on the active portion of the snail while the pads were pressurized, there was no detectable movement of the glass slide. When the snail was run using air there was detectable inflation under the microscope at 2.5 atmospheres however this inflation was so small that it did not produce the desired deflection necessary for the amplitude of a traveling wave.

After the cause of bubble formation was diagnosed, water replaced the air the fluid of choice to be pumped through the channels. The change in fluid reduced the observable channel inflation to only the first pad of channels in the three pad sets each input valve serviced. In fact, with water, the pressure had to be increased to 15 atmospheres of pressure to observe even this limited inflation. Since 15 atmospheres was the safety limit on the valves, pressure was not increased further. To better visualize how the fluid was actually filling the channels, food coloring was substituted for the water. This substitution yielded channel filling in a bell shaped curve fashion. This fill shape was in accordance to pressure loss in a long pipe, which was a good model for the behavior of the channels. Understanding that pressure drop needed to be minimized to insure channel inflation, a new set of designs was created.

4.2 Microsnail Iteration II

The new design's objective was to eliminate or at least minimize the pressure losses that were occurring in the original designs and create deflections in the elastomer detectable by finger touch. These new constraints resulted in designs of smaller snails with greater channel widths. One example of such a design is depicted in Figure 5.
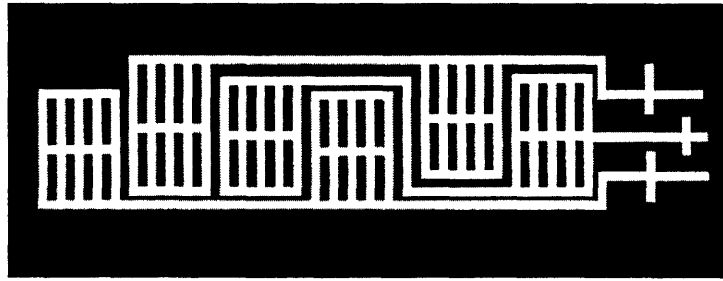
Figure 5 : The photo lithography mask of the new design. This figure is about twice as large as the actual snail to give a better picture of the channel design. The crosses on the right-hand side represent the location of the luer stub hole punches.

These snail designs displayed an active area of approximately 1cm by 4 cm and had channel widths of 500 micrometers. The 500 micrometer width was chosen based on the detectable inflation of the pneumatic input holes in the first iteration of snail design and testing. Another change was that the design was expanded from the nine pad design to include six pad and three pad designs. These simpler designs further reduced pressure loss by decreasing the length of channel through which water had to be pumped. Smaller active area designs of 0.5 and 0.7 cm by 4cm were also created, again in an attempt to reduce pressure losses by shortening net channel length by decreasing pad size.

Because the mold making process was altered for the new design, the first set of molds was defective. This failure was a result of failing to consider adequately the effect of the ratio between the height of the channels and the thickness of the channels. The five to one ratio allowed some of the smaller wavelengths to bleed into beyond the boundaries set by the mask which caused overexposure of the positive photo-resist. An attempt to try building a snail from the substandard molds resulted in a channel layer that would not remove from the mold and that tore when more force was applied in attempted removal. The diagnosis of the shear tearing that occurred in the faulty mold improved the process used in the baking of the next set of snails when new molds were produced. The same photolithography masks were used, but a filter was added during exposure of the photo-resist to remove the short wavelengths of light that were bleeding and thereby causing the overexposure in the original mold. The addition of the filter produced molds without any of the imperfections found in the first batch of the new design. Additionally, the extended bake time and application of fresh silane eliminated the shear tearing when the channel layer was removed from the mold.

4.3 Pressure Optimization Results

After building the new snails, it was necessary to test the effectiveness of the new design on eliminating the pressure drop problems with inflation. The pressure was stepped as explained in Section 3.2.3 and the channels were found to inflate and deflate in a repeatable fashion at 5 atmospheres. Two different membrane thicknesses were tested. At the ten micron thickness, the membrane was found to consistently rupture when pressure was applied while at the thirty micron thickness the membrane did not fail even at the maximum pressure of 13 atmospheres.

4.4 Snail Movement

Using the new design discussed in Section 4.2, the optimal pressure discussed in Section 4.3, and running Labview 6.1 so that the valves would cycle through every 2.4 seconds, the snail was placed in a Petri dish lined with a thin coating of silicon oil. Unfortunately, this did not produce movement. Postulating that the large amount of inactive surface surrounding the active channels might be producing enough drag to impede movement, the snail was turned upside down and a sliver of plastic transparency was placed over the inflating pads and a layer of silicon oil. Sure enough, the transparency was found to edge forwards at the end of each cycle at approximately $3.125 * 10^{-4}$ m/s. The set up that yielded this result is displayed in Figure 6.

Vise Grips to Hold Snail in
Upside down position

Transparency
on top of Snail

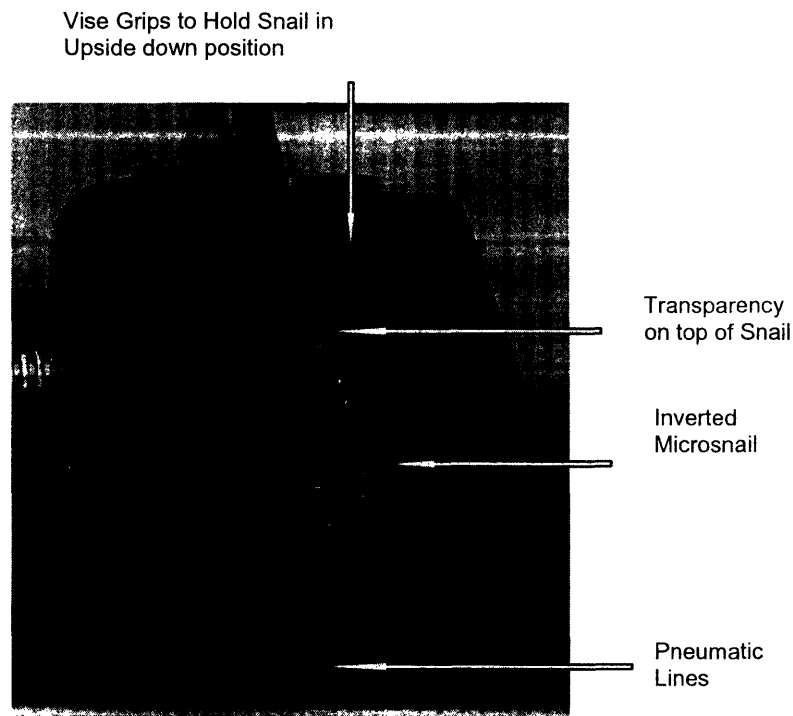Inverted
Microsnail

Pneumatic
Lines

Figure 6: Inverted Snail Set Up

Unfortunately, when the cycle time was increased, the elastomeric membrane exhibited cyclic failure and burst, and thereby rendered further observations on different net velocities in comparison to wave velocities impossible to test. This failure does leave the area open for further study.

5.0 Discussion

The breadth of complications surrounding the use of photolithography, pneumatics, and the chemistry surrounding the use of soft lithography for mechanical purposes present of a host of issues warranting discussion.

15

5.1 Causes for mold failure

When creating the molds, photolithography methods had to be used. The negative photo-resist, SU-8 2050, was particularly sticky and tended to be very difficult to move precisely via wafer tongs when transferring the coated wafer from spincoater, to hot plate, to oven or vice versa. Sometimes removing the wafer from the tongs would cause the wafer to become upended or fall to the side of the small spincoater platform causing contamination along the edges. The best remedy for this problem was to clean the tongs to remove any residual stickiness after every transfer of the wafers.

The SU-8 2050, also had a tendency to accumulate small airbubbles during the spincoating process which had to be popped using a razor edge. These airbubbles caused imperfections on the resist surface. There was no way to avoid these bubbles. Thus the mold masks were maneuvered around the imperfections to minimize their effect if not to keep the imperfections in the part of the mold eventually washed away by the developer.

These causes for mold imperfections may have resulted in a channel layers that were less precise and perhaps contributed to the lack of adequate adhesion between the membrane and channel layers.

5.2 Pressure losses and ramifications

As the small channels resulted in large pressure drops and subsequent inadequate fill the channels were also more robust since they did not deflect and undergo as much damage from cycling pressures. When the new design was implemented high pressures burst the channels that had previously withstood high pressures since active area for deflection was much smaller. Even at the optimum pressure the cyclic nature of the pressure input eventually led to channel failure. An improvement to this design might be to find a more robust polymer that could withstand more cycles before failure.

5.3 Moving from motors to pneumatics

Changes in drive mechanisms for any sort of locomotion are often rife with new problems and challenges. While, the first robosnail was larger, required moving plates, gearing, and motors, the induced wave pattern was independent of pressure losses, forces from pneumatic tubing, and issues of sufficient weight distribution. In the original snail the sinusoidal waves were continuous in contrast to the peristaltic stepping mechanism necessary in the pneumatic mechanism. In short, the pneumatic snail had more variables which deviated from nature and could be possible sources of failure.

5.4 Model predicted velocity ratio versus actual velocity ratio

Since the parameters of the snail were first determined by the mathematic model of the snail, it made sense to compare the ratio of the final experimental net velocity of the transparency to the wave velocity of the actual snail to the ratio found by the model. It turned out that there was considerable deviation between the expected and actual values of the ratio.

The model's ratio was 0.56 net/wave velocity. The actual ratio was .05 net/wave velocity. The difference by an order of magnitude could be attributed to the discontinuity of the pumping mechanism as opposed to the continuous nature of an actual traveling wave.

6.0 Conclusions and Recommendations

When considering questions of scale and the applications of models, the primary constraints in one situation may not be the primary constraints in another situation. In this attempted to recreate snail crawling using pneumatic peristaltic pumping, it was actually the premise that small channels could be instantly inflated that proved to be the most problematic. Getting the snail to move became the goal of the project as opposed to the original aims of attempting to visualize the flow layers around the crawling snail. Further work on this visualization could easily be the topic of further exploration. In fact the application of fluorescence to determine the height of thin films is a topic warranting discussion on its own merits.[9]

Designs with more than three phases for a pneumatic pumping mechanism that more closely approximated a continuous wave would also be interesting to evaluate the importance and effectiveness of the continuity of the traveling wave. One of the original designs which had eight inputs was not tested due to the inability to program a set of valve controls with easily adjustable speeds in the given time frame. Another challenge would be to create an artificial snail with as many wavelengths as found in real snails. The modeled snails all had no more than 4 wavelengths along its traveling wave and real snails have upwards of 15 wavelengths. [2]

Finally, along a non-mechanical avenue, it would interesting to develop a compound that imitated the properties of snail mucous which enables both adhesion and locomotion and could open new areas of research in the possibilities of machines that could crawl up walls. Some background work has already done in this area characterizing the ability of mucus to change from solid to liquid is a necessity for adhesive locomotion. There is a constant ratio between yield stress, the stress at which the mucous will snap apart like a solid, and flow stress, the stress at which the mucous will flow like a liquid. At set strains mucus will yield, but given a recovery time, of one second after yielding, where stress is removed, it will quickly heal again and behave as a solid. This repeatable 'yield-heal' could present very exciting new possibilities. [7]

7.0 Annotated References

[1] Denny, M.W. (1989). Invertebrate Mucous Secretions: Functional Alternatives to Vertebrate Paradigms. *Society for Experimental Biology,* 337-366.

Locomotion in snails, slugs and limpets is different from locomotion in other animals because they have only one foot, the great majority of them adhere to the surface on which they crawl, and from the dorsal view they appear to move without moving parts. The explanation of the adherence and gliding movement is found in two factors. The presence of mucus, and the waves that move in series along the ventral, also known as the pedal, portion of the foot work together to create forward locomotion.

In some snails, the waves move from the posterior to the anterior of the snail in the same direction as the net snail movement. This type of wave is called a direct wave. In other snails the waves move from the anterior to the posterior of the snail in the opposite direction of the net snail movement. This sort of wave is termed a retrograde wave. These waves cause forward motion by inducing various forces in the mucus. Thus, studying these forces and their reactions as the pedal wave moves can lead to better understandings of the mechanisms involved in gastropod locomotion.

Based on mucus properties, the upper limit on the crawling speed of an A. columbianus is 0.6 mm/s where the actual maximum speeds range from 0.8-2.3mm/s. Slugs should be limited to lengths of less than 8-12cm supporting the assertion that mechanical properties of pedal mucus may contribute to limits on slug size.

[2] Denny, M.W. (1981). A Quantitative Model For the Adhesive Locomotion of the Terrestrial Slug, *Ariolimax Columbianus. J. exp. Biol.* **91,** 195-217.

A typical slug weighs 15g and has a foot surface area of 15cm^2. The foot are determines the area of mucus overwhich the slug must move and thereby the frictional resistance to movement. For slugs above 5g the foot loading remains constant at a value of about 0.95g/cm^2. The wave pattern occupies the central 2/3 of the foot and the waveless areas form a rim. Thirteen to seventeen waves are present on the foot. A pedal wave is 0.05 cm long, 0.02 cm high at it's highest point and 0.2cm wide for a volume of $1*10^{-4}$ ml.

[3] Dickinson, M.H.(1999) Bionics: Biological insight into mechanical design. *PNAS.* **96,** 14208-14209.

Mimicking biologic structures is not always easy because not only are the materials and structures complex but the feedback systems which are used to create functionality are equally complicated. However, as the performance gap between biology and mechanical analogs shortens, engineering can increase the amount of inspiration it takes from Nature.

[4]Dickinson, M.H., et al.(2000). How Animals Move: An Integrative View. *Science.* **288**, 100-106.

Although an animal may appear to move forward at a steady speed, the forces it exerts on the environment are anything but constant. An overriding theme of animal locomotion is that propulsive forces vary with time and that kinetic energy can be stored in many different forms. For small organisms, viscous resistances in fluid can produce motion of the organism relative to the fluid as long as the organism's motion is assymetric.

[5] F. M. White, Fluid Mechanics, Fourth Edition, Boston: WCB/McGraw-Hill, 1999.

[6] S. H. Crandall, N.C. Dahl, T. J. Lardner, An Introduction to the Mechanics of Solids, Second Edition, The McGraw-Hill Companies, Inc. Primis Custom Publishing, 1999.

[7] Denny, M. W., and Gosline, J.M. (1980). The physical properties of the pedal mucus of the terrestrial slug, Ariolimax Columbianus. *J. exp. Biol.* **88**, 375-393.

The ability of mucus to change from solid to liquid is a necessity for adhesive locomotion. There is a constant ratio between yield stress and flow stress of approximately two. At a strain of 5-6 the mucus will yield, but given a recovery time, of one second after yielding, where stress is removed, it will quickly heal again and behave as a solid. This 'yield-heal' cycle is repeatable.

[8] Unger, M.A., Chou, H.P., et al. (2000). Monolithic Microfabricated Valves and Pumps by Multilayer Soft Lithography. *Science.* **288**, 113-116.

In multilayer soft lithography multilayer structures are constructed by bonding layer of elastomer. Each of these layers is separately cast from micro-machined molds. Each layer has an excess of one of the two component reactive molecules so when the layers are interfaced the excess molecules further curing causes the two layers to irreversibly bond. Much like a good weld joint is a strong as the component parts its joining, the strength of this interface equals the strength of the bulk elastomer. Most importantly for the actuation of microstructures, the alstomer is a soft material with a Young's modulus of approximately 750kPa allowing large deflections with small actuation forces. Monolithic elastomer valves can be actuated with speeds that allow for opening and closing at 100Hz and a time response of 1 ms. Peristaltic pumps formed by arranging three valves on a single channel had a maximum pumping rate of 75 Hz. Pumping rate was determined by measuring the distance traveled by a column of water in a thin(0.5 mm interior diameter) tubing with 100micrometer by 100 micrometer by 10 micrometer valves. The maximum pumping rate was 2.35 nL/s.

[9] Johnson, M.F.G., Schluter, R.A., Bankoff, S.G. (1997). Fluorescent imaging system for global measurement of liquid film thickness and dynamic contact angle in free surface flows. *Rev. Sci. Instrum.* **68(11)**, 4097-4102.

Fluorescent dye dissolved in a liquid flow can be used to outline liquid-gas free boundaries and, with digital imaging, can be used to observe quantitatively surface wave propagation and

pattern formation. Fluid depth measurements with a precision of +/- 0.02mm is obtained routinely in flows of several millimeters depth.

[10] Jose Aponte, Mechanical Engineering 2003 Senior Thesis

[11] Susan Ji, "Analytical and Numerical Study of Robosnail", Massachusetts Institute of Technology, Summer Project 2003

[12] Micosystems Technology Laboratories: Standard Operating Procedures Online
     <<http://www-mtl.mit.edu/mtlhome/3Mfab/sop.html>>

[13] " Negative Tone Photoresist Formulations 2035-2100," Online Microchem Manual.
     << http://www.microchem.com/products/pdf/SU8_2035-2100.pdf>>

Appendix A: Code used to model the snail [11]

C++ program performing Newton iteration to solve equations and determine dimensionless forms of h0 and vsnail:

```
//Newton.cpp: solves Newton iteration, outputs the exact h0 and vsnail values (dimensionless
form)

#include <iostream.h>
#include<conio.h>
#include <stdlib.h>
#include <math.h>
#include <stdio.h>
#include<fstream.h>


double integrator(double f(double x, double h0), double a, double b, double h0);
                    //integrates function
double f(double x, double h0); //the function in question (dimensionless form)
double f2(double x, double h0); //the function squared
double f3(double x, double h0); //the function cubed
double deriv(double f(double x, double h0), double x0, double h0);
                    //the derivative of the function
double Fx(double f(double x, double h0), double h0, double vsnail);
                    //the force in the x direction calculated
double Fy(double f(double x, double h0), double h0, double vsnail);
                    //the force in the y direction calculated
double df(double x);
                    //the derivative of the function
void calcX(double inv[4], double F[2], double x[2]);
                    //calculates the dx parameters in the Newton Solver Equation
void inverse(double J[4], double inv[4]); //the inverse of the Jacobian matrix calculated
void findJ(double h0, double vsnail, double J[4]); //finds the Jacobian matrix


//inputs that can be set

//constants relating to wavelength, function of movement
double lambda=4.572, a=.1778, vwave=1.778;       //dimensional parameters

//constants relating to fluid properties
double mu=15, rhoF=1.264;  //viscosity is mu, and rhoF is the density of the fluid

//constants relating to Robosnail physical properties
double mass=125.438, w=3.2512, l=13.97, Hs=2.5908;   //w, l, Hs refer to the dimensions of the
snail (dimensional form)
double weight=mass*980;
double rhoS=mass/(w*l*Hs);
double length=13.97;

//calculation constants
double drho=(rhoF-rhoS);
double H=sqrt((mu*vwave*lambda)/(drho*980*Hs));
double RTOL=0.001, ATOL=0.00001;
double divide=128;
int spin=128;
double epsilon=H/lambda;

int main()
{
 double h0=.9, vsnail=.5, F[2]={0}, vsnailtemp=.5;
                    //set the initial guesses for h0 and vsnail (dimensionless form)
                    //IMPORTANT: set the variable vsnailtemp as the same value as vsnail
                    //imperative in making the program work correctly
 double J[4]={0}, x[2]={0}, inv[4]={0}, a, b, i=0;
 double square1=0, square2=0;
 do
 {
  findJ(h0, vsnail, J);
  inverse(J, inv);
  F[1]=Fx(f, h0, vsnail);
```

```cpp
   F[2]=Fy(f, h0, vsnail);
   calcX(inv, F,x);
   vsnail=vsnailtemp;
   h0+=x[1];
   vsnail+=x[2];
   square1=x[1]*x[1];
   square2=x[2]*x[2];
   a=square1+square2;
   if(vsnail < 0)
   {
     vsnail=vsnail*-1;
   }
   if(h0<0)
   {
     h0=h0*-1;
   }
   b=RTOL*(vsnail*vsnail+h0*h0)+ATOL;
   cout << "dx h0: " << x[1] << " dx2 vsnail: " << x[2] << endl;
 }
 while(a>b);
 cout << "h0: " << h0 << endl;
 cout << "vsnail: " << vsnail << endl;
 getch();
 return 0;
}

void calcX(double inv[4], double F[2], double x[2])
{
 inv[1]*=-1;
 inv[2]*=-1;
 inv[3]*=-1;
 inv[4]*=-1;
 x[1]=inv[1]*F[1]+inv[2]*F[2];
 x[2]=inv[3]*F[1]+inv[4]*F[2];
}

void inverse(double J[4], double inv[4])
{
 double coeff=1/(J[1]*J[4]-J[2]*J[3]);
 inv[1]=coeff*J[4];
 inv[4]=coeff*J[1];
 inv[2]=coeff*-1*J[2];
 inv[3]=coeff*-1*J[3];
}

void findJ(double h0, double vsnail, double J[4])
{
 double dh=.01*h0, dv=.01*vsnail;
 J[1]=(Fx(f, h0+dh, vsnail)-Fx(f,h0, vsnail))/dh;
 J[2]=(Fx(f,h0, vsnail+dv)-Fx(f,h0, vsnail))/dv;
 J[3]=(Fy(f,h0+dh, vsnail)-Fy(f,h0, vsnail))/dh;
 J[4]=(Fy(f,h0, vsnail+dv)-Fy(f,h0, vsnail))/dv;
}

double Fx(double f(double x, double h0), double h0, double vsnail)
{
 double first=0, second=0, deltaf[128]={0}, x0=0, function[128]={0};
 double temp=0, Qstar;
 double pstar[128], dp[128];
 double force=0, tempforce[128]={0}, forcey=0;
 double constant=1+(0.5*(vsnail/vwave));
 double why;
 double s=h0+(a/H);
 ofstream output;
 output.open("c:/UROP Fluids pressure.txt", ios::out);
 first=integrator(f2, 0, length/lambda, h0);
 second=integrator(f3, 0, length/lambda, h0);
 Qstar=(first*constant)/(second); //for this set of values, Qstar=0.139278
 for(int x=0; x< spin; x++)
 {
     first=integrator(f2,0,(x*length)/(lambda*divide),h0);
```

22

```
     second=integrator(f3,0,(x*length)/(lambda*divide),h0);
     pstar[x]=12*constant*first-12*Qstar*second;
     output << pstar[x] << " " <<  endl;
 }
 for(int y=0; y<spin; y++)           //for graphing purposes, calculate dp/dx
 {
   dp[y]=12*f2((y*length)/(lambda*divide), h0)*constant-12*Qstar*f3((y*length)/(lambda*divide),
h0);
   output << dp[y] << endl;
 }
 for(int w=0; w<spin; w++)           //for graphing purposes, calculate the movement of the
function
 {
   function[w]=0.02*(f((w*length)/(lambda*divide), h0)-h0);
   output << function[w] << endl;
 }
 for(int z=0; z<spin; z++)
 {
   deltaf[z]=deriv(f, (z*length)/(lambda*divide), h0);
   output << deltaf[z] << endl;
 }
 for(int v=0; v<spin; v++)
 {

tempforce[v]=(pstar[v]*deltaf[v])+(0.5*dp[v]*f(v*(length/(lambda*divide)),h0))+(vsnail/vwave)*
(1./f(v*(length/(lambda*divide)),h0));
 }
 for(int u=1; u<spin; u++) //use composite trapezoidal rule to find total force
 {
   force+=((tempforce[u-1]+tempforce[u])/2.0)*((length/lambda)/divide);
   output << force << endl;
 }
 return force;
}


double Fy(double f(double x, double h0), double h0, double vsnail)
{
 double first=0, second=0, df[128]={0}, x0=0, function[128]={0};
 double temp=0;
 double Qstar, pstar[128], dp[128];
 double force=0, tempforce[128]={0}, forcey=0;
 double constant=1+(0.5*(vsnail/vwave));
 double s=h0+(a/H);
 ofstream output;
 output.open("c:/UROP Fluids/pressure.txt", ios::out);
 first=integrator(f2, 0, length/lambda, h0);
 second=integrator(f3, 0, length/lambda, h0);
 Qstar=(first*constant)/(second); //for this set of values, Qstar=0.139278
 for(int x=0; x< spin; x++)
 {
     first=integrator(f2,0,(x*length)/(lambda*divide),h0);
     second=integrator(f3,0,(x*length)/(lambda*divide),h0);
     pstar[x]=12*constant*first-12*Qstar*second;
     output << pstar[x] << " " <<  endl;
  }
 for(int y=0; y<spin; y++)           //for graphing purposes, calculate dp/dx
 {
   dp[y]=12*f2((y*length)/(lambda*divide), h0)*constant-12*Qstar*f3((y*length)/(lambda*divide),
h0);
   output << dp[y] << endl;
 }
 for(int w=0; w<spin; w++)           //for graphing purposes, calculate the movement of the
function
 {
   function[w]=0.02*(f((w*length)/(lambda*divide), h0)-h0);
   output << function[w] << endl;
 }
 for(int z=0; z<spin; z++)
 {
   df[z]=deriv(f,(z*length)/(lambda*divide),h0);
   output << df[z] << endl;
```

```cpp
}
for(int t=1; t<spin; t++)
{
  forcey+=((((pstar[t-1]+pstar[t])/2)*((length/lambda)/divide)))-((length/lambda)/divide);
//for composite trapezoidal rule, h=(b-a)/n=1/128
}
output << forcey << endl;
return forcey;
}


double deriv(double f(double x, double h0), double x0, double h0)
{
 double delta=.01;
 return (f(x0+delta, h0)-f(x0, h0))/delta;
}


double integrator(double f(double x, double h0), double a, double b, double h0)
{
 double h;
 double left=1, right=0, sum=0, sum2=0;
 int n=128;
 while(left>right)
 {
  sum2=sum;
  sum=0;
  h=(b-a)/n;
  for(int i=1; i<n; i++)
  {
   sum+=h*f(a+i*h, h0);
  }
  sum+=(0.5*h)*(f(a, h0)+f(b, h0));
  left=fabs(sum-sum2);
  right=RTOL*fabs(sum)+ATOL;
  n*=2;
 }
 return sum;
}


double f(double x, double h0)          //enter function here in dimensionless form
{
 return((a/H)*sin(2*3.14*(x))+h0);
}


double f2(double x, double h0)
{
 return 1/(f(x, h0)*f(x, h0));
}


double f3(double x, double h0)
{
 return 1/(f(x, h0)*f(x, h0)*f(x, h0));
}


double df(double x)
{
 return (a/H)*((2*3.14)*cos(2*3.14*x));
}
```
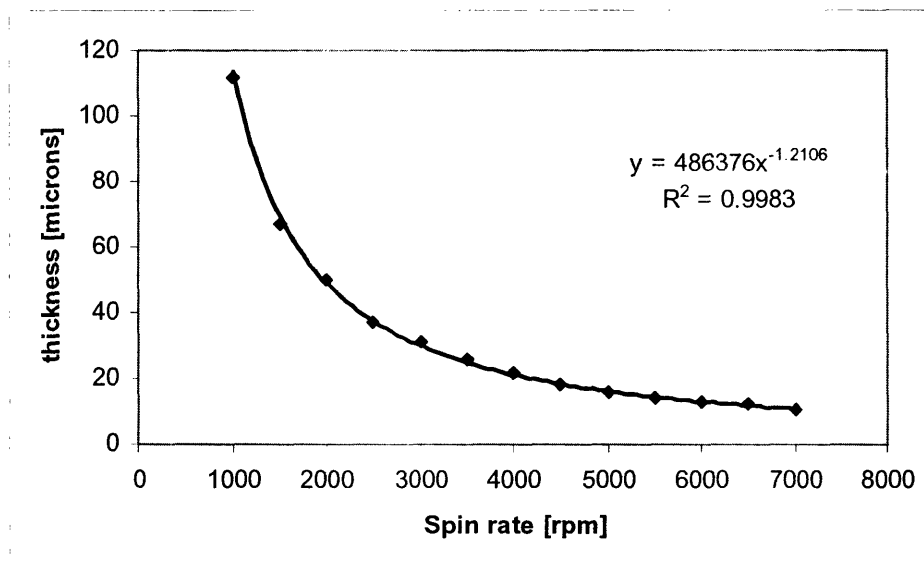
Appendix B: Soft Lithography Background Information

Mix Ratios:

        Channel Layer: 5 parts GE Silicon Rubber RTV615A (base material)

                        1 part GE Silicon Rubber RTV615B (catalyst for crosslinking)

        Membrane Layer: 20 parts GE Silicon Rubber RTV615A(base material)

                        1 part GE Silicon Rubber RTV615B(catalyst for crosslinking)

Chart to Determine Spin Coater Speed when creating Membrane Layer:

The chart plots thickness [microns] on the y-axis (0 to 120) against Spin rate [rpm] on the x-axis (0 to 8000), showing a decreasing curve.

$$y = 486376x^{-1.2106}$$
$$R^2 = 0.9983$$

[10]

Spin speeds used when attempting different membrane thicknesses:

- 1000 rpm
- 3000rpm
- 5000rpm

25

Appendix C: Peristaltic Pumping Capabilities of Labview 6.1

Labview 6.1 is a program that can be used to program circuit boards to act as control systems for valve switching of up to eight valves. The particular valve switching program written by doctoral student, Mats Howard Cooper, allows three valves to be turned on or off in repeatable cycles. The amount of overlap between the on and off cycle of each valve is determined by a range input by the user which must be set between 2 valves closed at all times to only 1 valve closed at a time.

When running the microsnail the switching overlap was set to 2 valves closed at a time to achieve a asymmetry necessary for forward motion. Since the peristaltic pump was found to work most effectively at 1.5 valves closed at a time or rather half cycle overlaps, this switching pattern would also be interesting to observe in later work.